INTERNATIONAL JOURNAL FOR NUMERICAL AND ANALYTICAL METHODS IN GEOMECHANICS
*Int. J. Numer. Anal. Meth. Geomech.*, **24**, 29–45 (2000)

# A SYMMETRICAL STREAMLINE STABILIZATION SCHEME FOR HIGH ADVECTIVE TRANSPORT

E. WENDLAND AND G. SCHMID

*Ruhr–Universität, Bochum, Germany*

## SUMMARY

An overview of numerical techniques and previous investigations related to the solution of advection-dominated transport processes is presented. In addition a new Symmetrical Streamline Stabilization ($S^3$) scheme is introduced. The basis of the technique is to treat the transport equation in two steps. In the first step the dispersion part is approximated by a standard Galerkin approach, while in the second step the advection is approximated by a least-squares method. The two parts are reassembled, resulting in one system of equations. The resulting coefficients' matrix is symmetric. Only half of a sparse matrix needs to be stored. Robust iterative algorithms for symmetrical systems of equations such as the preconditioned conjugate gradient method (PCG) can be successfully used. The new method leads to an implicit introduction of an 'artificial diffusion' term. Solute transport with high Peclet and Courant numbers does not lead to oscillations due to an inherent upwind damping. The upwind effect acts only in flow direction. The efficiency of the new formulation in terms of accuracy and computation time is shown in comparison with the Galerkin approach for mesh parallel and mesh oblique high advective solute transport. Copyright © 2000 John Wiley & Sons, Ltd.

KEY WORDS: upwind; finite element; transport; advection–diffusion; stabilization

## INTRODUCTION

Negative concentrations in the numerical solution of transport processes have no physical meaning and appear only because of spurious numerical oscillation inherent in the discretization schemes employed. This situation occurs mainly in processes that are described by the advection–dispersion equation. It originates from the presence of a first-order derivative in the governing equation, namely the advective term. Consequently, the governing equation has a hyperbolic or parabolic characteristic depending on the relative importance of advection and dispersion. For advection-dominated problems (hyperbolic character) the numerical computation has an unstable behaviour leading to unrealistic results. The solution of this problem by the traditional finite element approach becomes numerically inefficient. In order to avoid oscillations, a fine discretization is needed, leading to excessive requirements in terms of storage and computation time.

In this paper we present an overview of previous investigations and techniques for the solution of advection-dominated transport processes. The discussion is based on an application of a finite element procedure. In addition, a method aiming for numerical stability and computational savings is proposed in this work. According to the operator splitting technique described by

* Correspondence to: Professor E. Wendland, Lehrstuhl Angewandte Geol., Ruhr-Universitat, Raum NA 4/132, D-44780 Bochum, Germany. E-mail: ew@geol3.ruhr-uni-bochum.de

CCC 0363–9061/2000/010029–17$17.50
*Received 17 August 1998*
*Revised 25 January 1999, 22 March 1999*

Marchuk,[1] the governing equation will first be broken down into two parts. Extending the method of König,[2] the advective and dispersive terms will be approximated by different finite element techniques leading to a single system of equations. Although the advective term is considered in the implicit part of the equation the resulting coefficient matrix remains symmetric. Under this condition, a fast and robust preconditioned conjugate gradient method (PCG) similar to that proposed by Schmid and Braess[3] can be used. Another characteristic is the inherent presence of an 'upwinded' advection which ensures the stability of the numerical solution.

## GOVERNING EQUATION

We consider a single phase flow (e.g. water with a single dissolved solute) moving through a homogeneous, saturated porous medium. The flow field is independent of the solute concentration and is assumed to be at steady state. Chemical reactions and decay will not be considered, although this can easily be incorporated into the mathematical and numerical models.

In this case, the transient transport of dissolved solutes is governed by the advection–dispersion equation

$$\frac{\partial c}{\partial t} + \mathbf{v}\nabla c - \nabla(\mathbf{D}\nabla c) = Q\delta(c^{*} - c) \tag{1}$$

where $\mathbf{x}$ is the position vector, $t$ is the time, $c(\mathbf{x}, t)$ is the solute concentration, $\mathbf{v}(\mathbf{x})$ is the velocity vector, $\mathbf{D}(\mathbf{x})$ is the hydrodynamic dispersion tensor, consisting of the mechanical dispersion and molecular diffusion, $Q$ is a point source with concentration $c^{*}$ specified at the location $\mathbf{x}_0$ and $\delta(\mathbf{x} - \mathbf{x}_0)$ is the Dirac function.

## OVERVIEW

The methods used to stabilize the advection–dispersion can be divided into three fundamental groups: upwinding, Eulerian–Lagrangian approach and splitting-up. In the next sections we describe and discuss these methods.

### *Upwinding*

The idea of upwinding stems from the finite difference method. By the approximation of the advective term using central difference, the nodes upstream and downstream have the same weighting. By this means, the perturbations downstream have influence on the discrete approximation of the process upstream. As a result the numerical solution exhibits oscillations and instabilities. An improvement can be obtained using a backward approximation for the advective term. In the numerical formulation the upstream nodes are given a higher weighting (upwind). The technique can be seen as a central difference approximation with a superimposed artificial diffusion. Brooks and Hughes[4] showed that the approximation using central difference causes the appearance of negative artificial diffusion. The upwind is also a correction of an incorrect description of the physical process.

It is well known that the approximation with the Galerkin approach corresponds to a central-difference scheme. Therefore, the standard finite element method shows instability for high advective processes. The experience with upwind techniques for the finite difference method

 

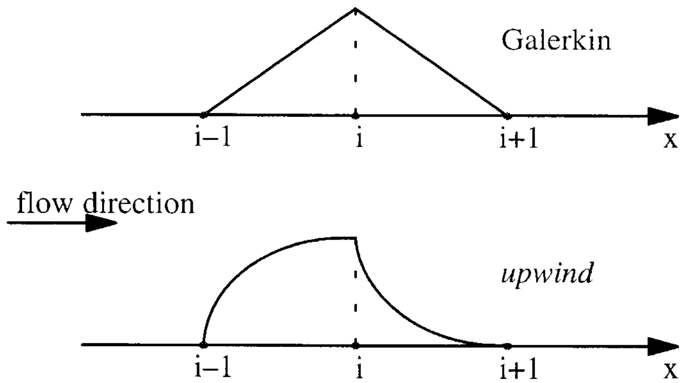


Figure 1. Comparison of Galerkin and upwind weighting function (Brooks and Hughes[4])

should be applied to the finite element method (FEM). The nodes upstream are strongly weighted using an unsymmetrical weighting function (see Figure 1). This procedure is known as Petrov–Galerkin weighting. The base function is modified by an additional term resulting in the unsymmetrical weighting function.

*Euler–Lagrange*

The second group of computational schemes considers the approximation of the transport equation from an Eulerian–Lagrangian point of view. A Eulerian approximation considers a fixed system of reference. Sharp concentration fronts cannot be well modelled. Such problems do not occur in the Lagrangian approximation while the reference frames move with the particles. The missing mesh leads to other problems mainly for heterogeneous regions, singularities (wells and sinks) and irregular boundaries. The drawbacks of each approximation can be overcome using a combined scheme.

Introducing the material derivative

$$\frac{Dc}{Dt} = \frac{\partial c}{\partial t} + \mathbf{v}\nabla c \tag{2}$$

the transport equation (1) can be rewritten in a Lagrangian form

$$\frac{Dc}{Dt} - \nabla(\mathbf{D}\nabla c) = Q\delta(c^* - c) \tag{3}$$

The solution of the transport problem can now be divided in two parts: a hyperbolic one (equation (2)) for the advection and a parabolic one (equation (3)) for the hydrodynamic dispersion and other processes.

The advective part is usually described along a characteristic curve. The material derivative for a moving coordinate system with velocity

$$\mathbf{v} = \frac{D\mathbf{x}}{Dt} \tag{4}$$

 

Table I. Summary of related work

| Authors | Year | Characteristics |
|---|---|---|
| *Upwind* | | |
| Hughes[5] | 1978 | Unsymmetrical weighting function changes only the advective term |
| Kelly *et al.*[6] | 1980 | Balancing dissipation also occurs perpendicular to flow direction (cross diffusion) |
| Brooks and Hughes[4] | 1982 | Upwind appears only in flow direction with SUPG (streamline upwind/Petrov–Galerkin) |
| Hughes and Brooks[7] | 1982 | Consistency analysis for SUPG |
| Hughes[8] | 1987 | Overview of advances of SUPG for the analysis of the Navier–Stokes equations |
| Hughes *et al.*[9] | 1987 | Convergence and error estimation of SUPG for the advection–dispersion equation |
| Tezduyar *et al.*[10] | 1987 | SUPG method for the advection–diffusion–reaction equation |
| DoCarmo and Galeão[11] | 1991 | Artificial diffusion only for sharp concentration gradients and discontinuities |
| Leismann and Frind[12] | 1989 | Optimal upwind through an error analysis with implicit dispersion and explicit advection |
| Gärtner[13] | 1987 | Optimal upwind through error analysis for the density-dependent transport equation |
| Kröhn[14] | 1990 | Higher consistency for problems of fractured porous media |
| Huyakorn and Pinder[15] | 1983 | Further discussion of upwind techniques |
| Voss[16] | 1984 | Upwind application to practical problems |
| Huyakorn *et al.*[17] | 1983 | Upwind application to practical problems |
| Helmig[18] | 1993 | Petrov–Galerkin for multiphase flow in a fractured medium |
| Carrano and Yeh[19] | 1994 | Optimization of upwind term based on a Fourier analysis |
| *Euler-Lagrange* | | |
| Neuman[20] | 1984 | Basic discussions of the Eulerian–Lagrangian approach and applications of praticle tracking |
| Kinzelbach[21] | 1987 | Particle tracking applications |
| Szymkirewicz[22] | 1993 | Spline functions for determination of the characteristics |
| Blömer[23] | 1992 | Discretization scheme for practical transport problems with point sources or sinks (wells) |
| Garder *et al.*[24] | 1964 | Method of characteristics (MOC) for the simulation of oil prospecting |
| Konikov and Bredehoeft[25] | 1978 | Popularization of the method of characteristics (MOC) |
| Ijiri and Karasaki[26] | 1994 | Time-dependent adaptive mesh generation for dispersion using the finite element method |
| Celia[27] and Binning and Celia[28] | 1994 | Solute mass conservation for finite volumes using ELLAM (Eulerian–Lagrangian Localized Adjoint-Methods) |
| Ewing *et al.*[29] | 1994 | Coupled simulation of fluid, heat and radioactive transport using ELLAM |
| Hinkelmann and Zielke[30] | 1995 | Flow and salt transport on shadow systems |
| *Operator split* | | |
| Marchuk[1] | 1975 | Mathematical description of the operator split technique |
| Marchuk[31] | 1995 | Overview of different splitting-up techniques |
| Douglas and Rachford[32] | 1956 | Heat transport using the Alternating Direction Implicit (ADI) scheme |
| Szymkiewicz[22] | 1993 | Operator splitting for the transport equation |

 

Table I. Continued

| Authors | Year | Characteristics |
|---|---|---|
| König[33] | 1991 | Splitting technique applied to the transport equation leading to a symmetric system of equations |
| Morshed and Kaluarachchi[34] | 1995 | Operator splitting procedure applied to the advection–dispersion reaction equation |

is for the advective part equal to zero:

$$\frac{Dc}{Dt} = 0 \tag{5}$$

Physically this implies that the concentration of a solute moving along a characteristic curve does not change. The characteristic curve, however, has to be determined. Particle tracking is the most frequently used technique. The path described by solute particles in the flow field is along the streamlines. The particles can be followed forward, backward and by a combination of both. The second part of a time step is concerned with the solution of the dispersion equation. The new concentration distribution is superimposed upon the advective one.

The application of the Eulerian–Lagrangian method to transient flow fields is limited. For time–dependent cases the determination of the characteristic curve is ambiguous. The pathlines can cross each other due to changes in time in the hydraulic gradient.

### *Operator splitting techniques*

The operator splitting techniques have been developed parallel to the separation of advection and dispersion according to a Eulerian–Lagrangian scheme. Complex mathematical problems can be separated into single operators and treated separately (Marchuk[1,31]). This mathematical technique can be applied to many different physical processes. For the advection–dispersion equation, this leads to the same effect as the Eulerian–Lagrangian approach: a separation of advection and diffusion. The idea originates from the research in the 1950s dealing with the calculation of heat transport using the finite difference method.

Table I gives a symmary of some previous work related to the techniques described above.

## THE PROPOSED SCHEME

In this chapter a method aiming for numerical stability and computational efficiency is proposed. The mathematical development of the scheme is based on the operator splitting procedure. The numerical approximation by finite element techniques leads to a single symmetrical system of equations with an inherent upwind effect.

### *Operator splitting procedure*

The differential equation (1) can be discretized in time considering a first-order finite difference approach with the weighting factor $\theta$

$$\frac{(c^{+} - c^{-})}{\Delta t} + \theta(L_1 + L_2)c^{+} + (1 - \theta)(L_1 + L_2)c^{-} = f \tag{6}$$

 

where $c^+$ is the solute concentration at time level $(t + \Delta t)$, $c^-$ the solute concentration at time level $(t)$, $\Delta t$ the time step, $L_1 = -\nabla(\mathbf{D}\nabla) + Q\delta$, $L_2 = \mathbf{v}\nabla$, $f = Q\delta\, c^*$.

We introduce the dispersive component $c^{\mathrm{d}}$ of the concentration as a temporary unknown. According to Marchuk,[1] equation (6) can be broken down into a dispersive part, which depends only on the linear operator $L_1$

$$\frac{c^{\mathrm{d}}}{\Delta t} + \theta L_1 c^{\mathrm{d}} = \frac{c^-}{\Delta t} - (1-\theta) L_1 c^- + f \tag{7}$$

and an advective part, which depends on the linear operator $L_2$

$$\frac{c^+}{\Delta t} + \theta L_2 c^+ = \frac{c^{\mathrm{d}}}{\Delta t} - (1-\theta) L_2 c^{\mathrm{d}} \tag{8}$$

The spatial derivatives will be discretized following the technique proposed by König.[2] The exact solution for each step will be approximated by means of the finite element method using the standard interpolation scheme

$$c(x, y, z, t) \simeq \sum_{j=1}^{N} \varphi_j(x, y, z) c_j(t) \tag{9}$$

in which $\varphi_j$ is a linear base function.

*Dispersive term*

For the dispersive part given in equation (7), the solution is obtained by using the standard Galerkin approach. The minimum is obtained by weighting the residual with respect to the test function $\varphi_i$

$$\int_\Omega \varphi_i \left[ \frac{\Sigma \varphi_j c_j^{\mathrm{d}}}{\Delta t} + \theta L_1 \Sigma \varphi_j c_j^{\mathrm{d}} \right] \mathrm{d}\Omega = \int_\Omega \varphi_i \left[ \frac{\Sigma \varphi_j c_j^-}{\Delta t} - (1-\theta) L_1 \Sigma \varphi_j c_j^- + f \right] \mathrm{d}\Omega \tag{10}$$

which can be rewritten in matrix form as

$$\left( \frac{\mathbf{M}}{\Delta t} + \theta \mathbf{B} \right) c^{\mathrm{d}} = \left[ \frac{\mathbf{M}}{\Delta t} - (1-\theta)\mathbf{B} \right] c^- + \mathbf{F} \tag{11}$$

with

$$\mathbf{M} = \int_\Omega \varphi_i \varphi_j \, \mathrm{d}\Omega,$$

$$\mathbf{B} = \int_\Omega \mathbf{D}\, \nabla\varphi_i \nabla\varphi_j \, \mathrm{d}\Omega + \int_\Omega Q\delta\, \varphi_i \varphi_j \, \mathrm{d}\Omega,$$

$$\mathbf{F} = \int_\Omega Q\delta\, c^* \varphi_i \, \mathrm{d}\Omega.$$

 

*Advective term*

The advective part given in equation (8) can be solved by means of the least-squares method. The residual of the approximation will be minimized, weighting it with the test function

$$\frac{\varphi_i}{\Delta t} + \theta \mathbf{v} \nabla \varphi_i$$

$$\int_\Omega \left(\frac{\varphi_i}{\Delta t} + \theta \mathbf{v} \nabla \varphi_i\right)\left[\frac{\Sigma \varphi_j c_j^+}{\Delta t} + \theta L_2 \Sigma \varphi_j c_j^+\right] \mathrm{d}\Omega = \int_\Omega \left(\frac{\varphi_i}{\Delta t} + \theta \mathbf{v} \nabla \varphi_i\right)\left[\frac{\Sigma \varphi_j c_j^{\mathrm{d}}}{\Delta t} + (1-\theta) L_2 \Sigma \varphi_j c_j^{\mathrm{d}}\right] \mathrm{d}\Omega \quad (12)$$

In matrix form operation (12) yields:

$$\left[\frac{\mathbf{M}}{\Delta t} + \theta(\mathbf{V} + \mathbf{V}^{\mathrm{T}}) + \mathbf{U}^*\right] c^+ = \left[\frac{\mathbf{M}}{\Delta t} - (1-\theta)\mathbf{V} + \theta \mathbf{V}^{\mathrm{T}} - \frac{(1-\theta)}{\theta} \mathbf{U}^*\right] c^{\mathrm{d}} \quad (13)$$

where

$$\mathbf{V} = \int_\Omega \mathbf{v} \varphi_i \nabla \varphi_j \, \mathrm{d}\Omega;$$

$$\mathbf{U}^* = \theta^2 \Delta t \int_\Omega \mathbf{v}^{\mathrm{T}} \mathbf{v} \, \nabla \varphi_i \nabla \varphi_j \, \mathrm{d}\Omega.$$

*Symmetrical Streamline Stabilization ($S^3$)*

The traditional procedure of the splitting technique is to solve equation (11) and then substitute the temporary concentration $c^{\mathrm{d}}$ into the equation (13) getting the desired solution at the new time level. This substitution can be done analytically.[35]

The vector $\mathbf{M}/\Delta t \, c^{\mathrm{d}}$ appears in both expressions (11) and (13) through which they can be coupled to one equation. After extrapolation for elimination of the temporary concentration $c^{\mathrm{d}}$ the following assembled form of the governing equation results:

$$\left[\frac{\mathbf{M}}{\Delta t} + \theta(\mathbf{B} + \mathbf{V}) + \theta \mathbf{V}^{\mathrm{T}} + \mathbf{U}^*\right] c^+ = \left[\frac{\mathbf{M}}{\Delta t} - (1-\theta)(\mathbf{B} + \mathbf{V}) + \theta \mathbf{V}^{\mathrm{T}} - \frac{(1-\theta)}{\theta} \mathbf{U}^*\right] c^- + F \quad (14)$$

The analysis of equation (14) shows the advantages of the method. Using the least-squares method, the resulting coefficient matrix is always symmetric, even when the advective term appears in the implicit side of the equation. The symmetry is due to the presence of the term $\theta \mathbf{V}^{\mathrm{T}} c^+$ on the left-hand side of the equation.

Another characteristic is the upwind effect on the advective term, which is responsible for the stabilization of the numerical solution. It results from the combination of the terms $\mathbf{V}$ and $\mathbf{U}^*$, as shown in Figure 2.

This upwind term $\mathbf{U}^* = \theta^2 \Delta t \mathbf{v}^2$ can be interpreted in terms of the stability criteria for the one-dimensional case. Considering the Courant number $C_0 = v\Delta t/\Delta l$, the one-dimensional case can be transformed to the form

$$\mathbf{U}^* = \theta^2 C_0 \Delta l v \quad (15)$$

After introduction of the Peclet number $P_e = v\Delta l/D$ one achieves:

$$\mathbf{U}^* = \theta^2 C_0 P_e D \quad (16)$$

 

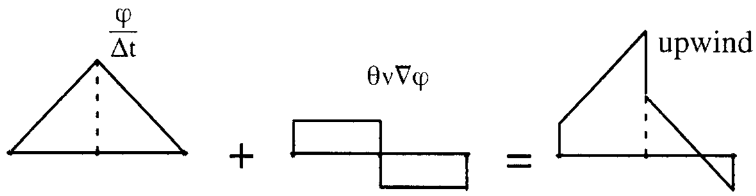


Figure 2. Weighting function for the advective term (modified from König[33])

The upwind term appears to be a scale-up of the natural dispersion of the problem, through which the numerical computation is stabilized avoiding spurious oscillation. In the $S^3$-procedure the artificial diffusion introduced by the numerical method is controlled by the time ($\theta$, $C_0$) and the spatial ($P_e$) discretization. In the SUPG scheme only the spatial discretization is considered.

Due to the dependence of the artificial stabilization on the flow field, a problem with cross diffusion will not be expected. This feature can be demonstrated for a two-dimensional example. Consider the arbitrary element $\Omega_e$ on a stationary flow given in Figure 3. Related to the global co-ordinate system $(x, y)$ the velocity vector $v$ is inclined with an angle $\gamma$.

The matrix of artificial diffusion for the global co-ordinate system is given as

$$U^*(x, y) = \theta^2 \Delta t \begin{bmatrix} v_x^2 & v_x v_y \\ v_x v_y & v_y^2 \end{bmatrix} \tag{17}$$

with $v_x = v \cos\gamma$ and $v_y = v \sin\gamma$

$$U^*(x, y) = v^2 \theta^2 \Delta t \begin{bmatrix} \cos^2\gamma & \sin\gamma\cos\gamma \\ \sin\gamma\cos\gamma & \sin^2\gamma \end{bmatrix} \tag{18}$$

where $v$ is the magnitude of the flow vector.

The relation

$$U^*(\xi, \eta) = T^{\mathrm{T}} U^*(x, y) T \tag{19}$$

with

$$T = \begin{bmatrix} \cos\gamma & -\sin\gamma \\ \sin\gamma & \cos\gamma \end{bmatrix} \tag{20}$$

can be used to transform the matrix to a local co-ordinate system $(\xi, \eta)$ with axes parallel and perpendicular to the velocity vector. Applying this mathematical operation to the matrix of artificial diffusion in equation (18) it results in

$$U^*(\xi, \eta) = \theta^2 \Delta t \begin{bmatrix} v^2 & 0 \\ 0 & 0 \end{bmatrix} \tag{21}$$

Due to the vector product $\mathbf{v}^{\mathrm{T}}\mathbf{v}$, the stabilization acts only in flow direction, avoiding the appearance of cross diffusion. The transformation can be derived for any coordinate system and is also applicable to three-dimensional problems.

A comparison of the developed scheme (equation (14)) with a traditional weighting residual method using an unsymmetrical weighting function for all terms leads to the observation that

 

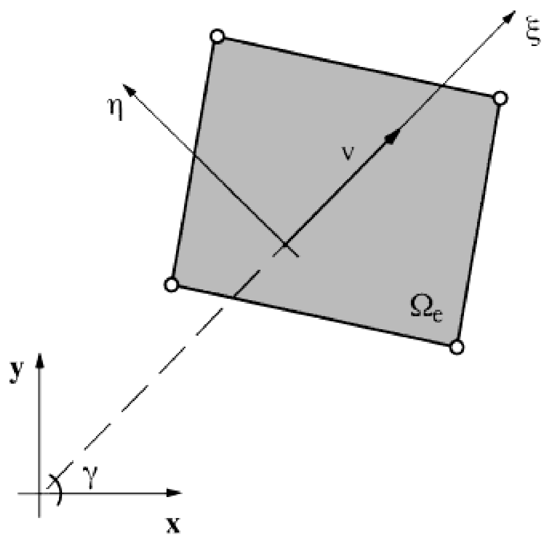


Figure 3. Arbitrary element in a given flow field

some higher-order derivatives (e.g. diffusion terms) are missing in the actual approximation. Nevertheless, Brooks and Hughes[4] showed if rectangular elements with linear interpolation functions are chosen, then the unsymmetric part of the weighting function does not affect the diffusion terms. Consequently the higher-order derivatives naturally vanish and would not affect the results. The proposed scheme is also consistent with the physical problem. This is not generally the case for quadratic or cubic interpolation functions for which the higher-order terms can be significant. In advection-dominated situations although one can also neglected these contributions.

Another important characteristic is the behaviour of the method for divergence free flow fields. In this case the symmetrization leads to an explicit approximation of the advective term and oscillation can be expected for high Courant numbers. As it will be shown in the applications the oscillation does not occur due to the stabilization generated by the upwind effect.

## APPLICATIONS

The efficiency of the presented method is demonstrated for two test cases. In the first one the flow is parallel to the discretization mesh. In the second one the flow is diagonal to the mesh discretization.

### *Mesh parallel flow*

The system consists of a uniform horizontal flow in a rectangular domain with a continuous contaminant source placed on the upstream boundary. The boundary conditions are shown in Figure 4.

The analytical solution given by Leij and Dane[36] is used as a reference solution for the $S^3$ and the standard Galerkin approach. We solve the problem with initial condition $c = 0$ over all the

 

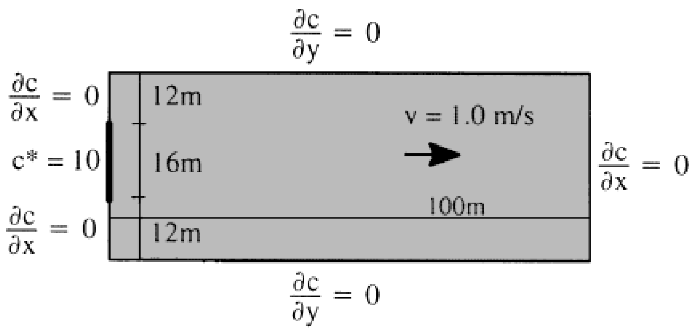


Figure 4. Test case for mesh parallel flow

domain using a regular mesh for different values of Peclet and Courant numbers up to a time $t = 50$ s. The time discretization was weighted with $\theta = 1{\cdot}0$ (implicit Euler method). The parameters used for the different cases are given in Table II.

In the first case, the transport is diffusion dominated and of parabolic character. The stability criteria ($P_e < 2{\cdot}0$ and $C_0 < 1{\cdot}0$) are observed. The numerical solutions of this problem with the $S^3$ and the standard methods are well behaved and agree with the analytical results (Figure 5). Figure 6 shows the break-through curves for a point located at $x = 6{\cdot}0$ and $y = 24{\cdot}0$ m. The curve for the $S^3$ method appears to be slightly closer to the analytical result.

In the second case, the transport is advection-dominated and of hyperbolic character. In order to get acceptable results a fine discretization has to be chosen. The stability criteria are not adhered to. In this situation difficulties due to numerical dispersion can be expected. The computed results are presented in Figure 7. Compared to the analytical solution, a higher longitudinal spreading can be observed for both numerical schemes. For the Galerkin method a negative concentration outside the plume and a broader spreading front can be observed. The corresponding break-through curves for a point located at $x = 6{\cdot}0$ and $y = 24{\cdot}0$ m are shown in Figure 8.

In a first evaluation, the major advantage of the $S^3$ scheme in comparison with the standard method appears to be the saving on computational effort. In Table III a comparison of storage requirements and computation time after 50 time steps for a mesh with 16 281 nodes is shown.

The Galerkin method leads to an unsymmetrical matrix, for which a direct solver was chosen. The full matrix has to be stored using a *banding technique* (with M as bandwith). For the $S^3$ scheme a robust preconditioned conjugate gradient solver (PCG) with *sparse storage* can be used. The saving in computer memory for large models ($M \gg 15$) is evident.

The computation time (CPU) given in Table III relates to a workstation RISC6000/550 (24,8 MFLOPS). The time consumed by our method is approximately 6 per cent of the traditional case. Although conjugate gradient solvers exist for unsymmetrical matrices, they are not so robust and efficient as the symmetric one. Therefore, the unsymmetrical solvers have not been considered.

*Mesh oblique flow*

The system consists of a rectangular domain uniformly discretized. The flow field is diagonal oriented. A continuous contaminant source is placed on the upstream boundary as shown in Figure 9. The remaining conditions are given as no flux over the boundary. All dimensions are

 

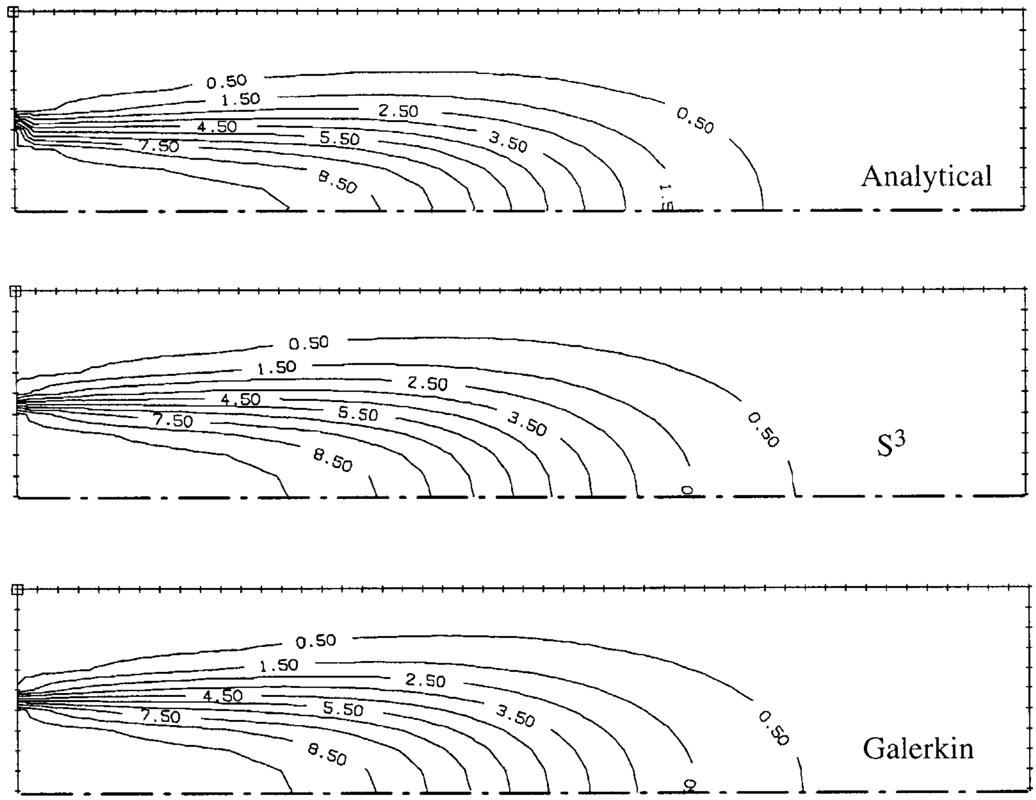


Figure 5. Concentration distribution for case 1 (only half part due to symmetry)

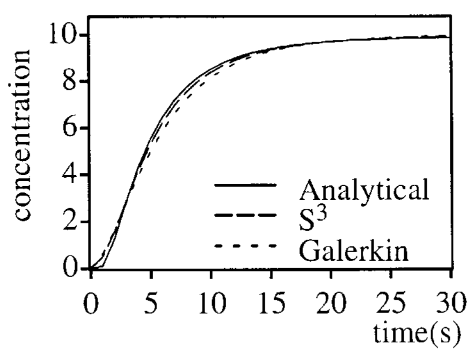


Figure 6. Break-through curves for case 1

in [m]. Considering a conductivity of $K = 100{\cdot}0$ m/s the flow equation leads to an average velocity of 1·5 m/s, which was used to compute the Courant and Peclet numbers.

The results obtained with the proposed method ($S^3$) are compared with the standard Galerkin approach (G). For this transport problem there is no analytical solution and the convergence of

 

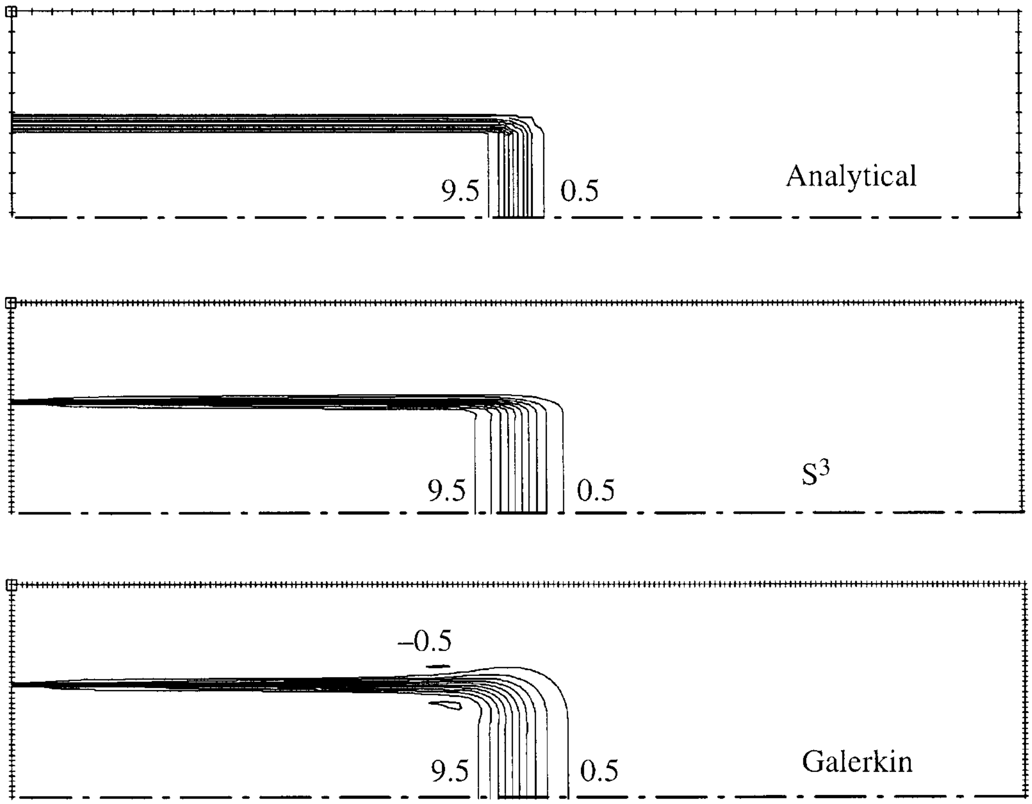


Figure 7. Concentration distribution for case 2 (only half part due to symmetry)

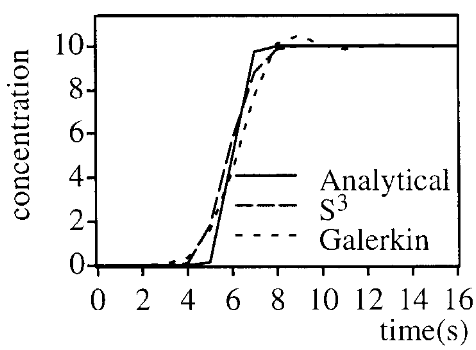


Figure 8. Break-through curves for case 2

the methods to the correct solution is achieved by refining the mesh. The problem is solved with the initial condition $c = 0$ over all the domain using a regular mesh for different values of Peclet and Courant numbers up to the time $t = 40$ s. The time discretization was weighted with $\theta = 1{\cdot}0$ (implicit Euler method). The parameters used for the different cases are shown in Table IV.

Table II. Discretization parameters for the example with mesh parallel flow

| Case | $\Delta t$ (s) | $D_L$ ($m^2/s$) | $D_T$ ($m^2/s$) | $\Delta x = \Delta y$ (m) | $P_e$ | $C_0$ |
|---|---|---|---|---|---|---|
| 1 | 1·0 | 2·0 | 0·2 | 2·0 | 1·0 | 0·5 |
| 2 | 0·1 | 0·02 | 0·002 | 0·5 | 25·0 | 0·2 |

$D_L$ = longitudinal, $D_T$ = transversal dispersion

Table III. Storage and CPU-time requirements for the test case with mesh parallel flow

| | Galerkin | $S^3$ |
|---|---|---|
| Storage | $M \times N$ | $15 \times N$ |
| CPU-time (s) | 5000·0 | 300·0 |

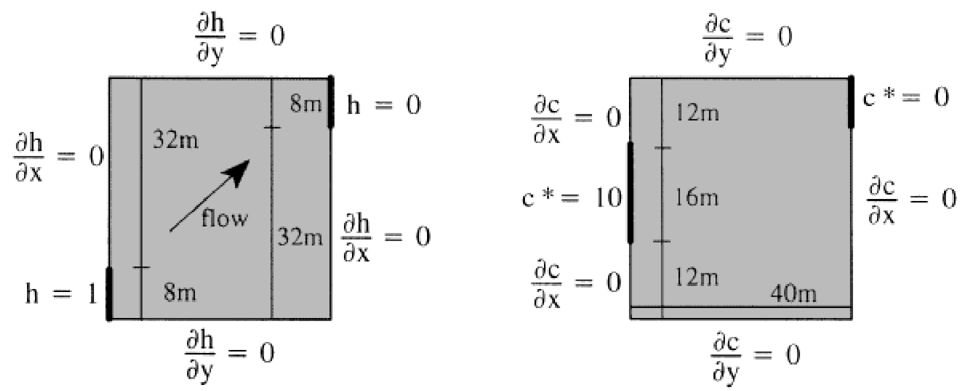


Figure 9. Test case for mesh oblique flow: a. flow (with h as hydraulic potential), b. transport

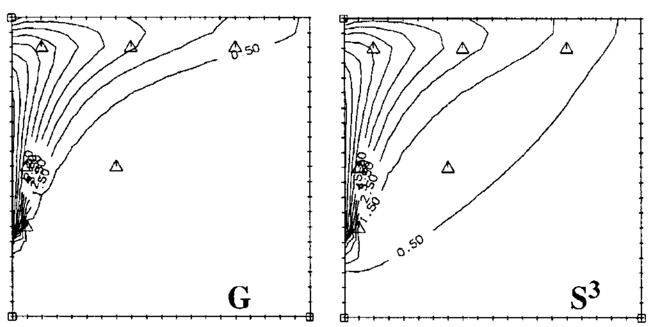


Figure 10. Concentration distribution for case III

The triangles in Figures 12–15 are spatial references in order to compare the numerical concentration distributions.

In the first case (III), the transport is diffusion dominated and of parabolic character. The stability criteria ($P_e < 2{\cdot}0$ and $C_0 = 1{\cdot}0$) are nearly observed. The numerical solution of this

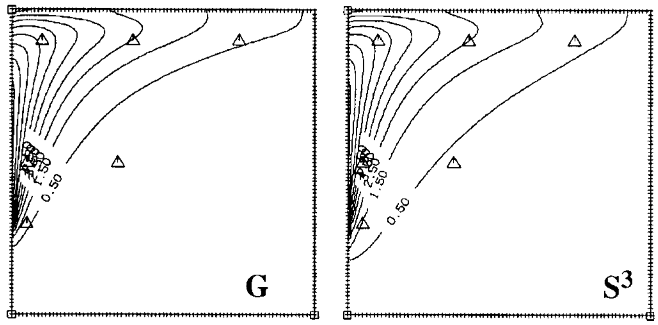


Figure 11. Concentration distribution for case IV

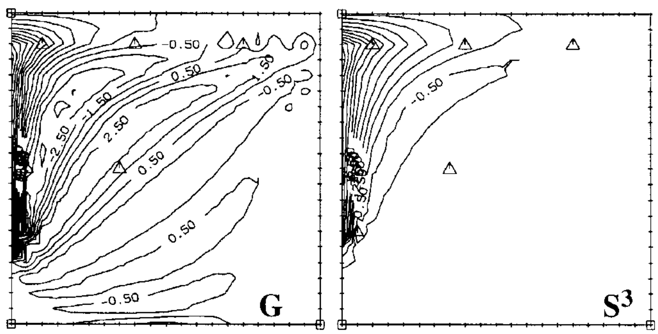


Figure 12. Concentration distribution for case V

problem with the S$^3$-scheme is well behaved (Figure 10) and approximates the Galerkin results, although one can observe the increased numerical diffusion due to upwind effects. As shown in equation 16 the upwind represents an upscaling of the natural diffusion depending on the Peclet and Courant numbers. For the given case with mesh oblique flow this artificial diffusion appears to be over-dimensioned. After mesh refinement for case IV, the result with the S$^3$-scheme converges with the solution with the traditional method (Figure 11). For diffusion dominated problems the proposed scheme may need a correction factor in order to reduce the artificial diffusion.

For case V the transport is advection dominated and hyperbolic in character. Because of the discretization chosen, the stability criteria are not adhered to ($P_e \gg 2{\cdot}0$). In this situation difficulties due to numerical dispersion can be expected. The computed concentration distributions after 40 s are shown in Fig. 12. The Galerkin method presents serious numerical problems due to the high Peclet number. The results oscillate strongly, resulting in an unreliable solution. For the S$^3$-scheme the problem does not occur, due to the oscillation damping created by upwind.

For case VI the mesh is refined and the result for the standard method (G) agrees with the S$^3$-scheme (Figure 13). The details show the concentration distribution in a region upstream from the solute sources. For the Galerkin scheme the negative values growth up to $-8{\cdot}5$. This problem does not occur with the S$^3$-scheme. It merely remains an isoline

 

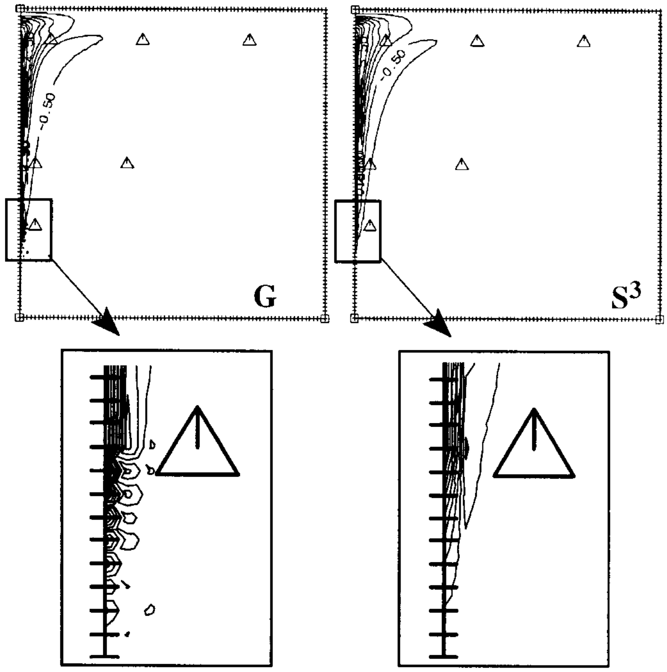


Figure 13. Concentration distribution for case VI

Table IV. Discretization parameters for the example with mesh oblique flow

| Case | $\Delta t$ (s) | $D_L$ ($m^2$/s) | $D_T$ ($m^2$/s) | $\Delta x = \Delta y$ (m) | $P_e$ | $C_0$ |
|---|---|---|---|---|---|---|
| III | 2·0 | 2·0 | 0·2 | 2·0 | 1·0 | 1·5 |
| IV | 1·0 | 2·0 | 0·2 | 0·5 | 0·25 | 3·0 |
| V | 1·0 | 0·02 | 0·002 | 2·0 | 100·0 | 0·75 |
| VI | 1·0 | 0·02 | 0·002 | 0·5 | 25·0 | 3·0 |

Table V. Storage and CPU-time requirements for the test case with mesh oblique flow

| | Galerkin | $S^3$ |
|---|---|---|
| Storage | $M \times N$ | $15 \times N$ |
| CPU-time (s) | 3296·0 | 110·0 |

with negative concentration (−0·50), which appears due to the difficult numerical condition of this case.

In Table V a comparison of storage requirements and computation time after 40 time steps for a mesh with 64000 nodes is shown.

## CONCLUSION

The Symmetrical Streamline Stabilization ($S^3$) scheme has been introduced, providing a robust algorithm to solve the advection–dispersion equation, even for advection-dominated problems. Starting with an operator splitting procedure, the method leads to a single symmetric coefficient matrix with the advective term being considered in the implicit part of the equation. As a consequence, a symmetric preconditioned conjugate gradient solver can be used. Furthermore, the advective term is upwinded, ensuring a stable solution without numerical oscillation, even for high advective transport. In a test case with mesh parallel transport, the proposed method was demonstrated to be slightly more accurate than the standard approach, either for advection- or dispersion-dominated transport. For an application with mesh oblique transport the Galerkin method failed for high Peclet numbers while the $S^3$ scheme remains stable due to the positive effect of the upwind term along the streamlines.

The results presented here allow the following conclusion: for high advective transport problems in mesh oblique flow the standard finite element method leads to numerical problems with spurious oscillation. By refining the mesh, this problem can be overcome, but the numerical effort increases. The Symmetrical Streamline Stabilization ($S^3$) scheme presents a good alternative reaching at least the same results as the traditional Galerkin method. It proves to be a robust algorithm for solving the advection–dispersion equation, both for advection- and for dispersion-dominated problems. In test cases for advection-dominated transport the method presented has been demonstrated to be more accurate than the standard approach. The major advantage of the proposed method appears to be the saving in computational effort. Both the computation time and storage needs could be significantly reduced. For the S3-scheme a robust preconditioned conjugate gradient solver (PCG) with *sparse storage* can be used. The saving in computer memory for large models ($M \gg 15$) is significant. The time consumed by the new method is considerably smaller than for the standard case. Although conjugate gradient solvers exist for unsymmetrical matrices, they are not so robust and efficient as a symmetic one.

In a future work we will assign the application of the $S^3$-scheme for practical problems concerning the spread of solutes in a fractured porous medium in the vicinity of an underground repository.

## REFERENCES

1. G. I. Marchuk, *Methods of numerical Mathematics*, Springer, New York, 1975.
2. C. König, 'Operator split for three dimensional mass transport equation', *Proc. Computational Methods in Water Resources X*, Vol. 1, Heidelberg, 1994, pp. 309–316.
3. G. Schmid and D. Braess, 'Comparison of fast equation solvers for groundwater flow problems', *Proc. Groundwater Flow and Quality Modelling*, Reidel, Dordrecht, 1988, pp. 173–188.
4. A. N. Brooks and T. J. R. Hughes, 'Streamline upwind/Petrov–Galerkin formulations for convection dominated flows with particular emphasis on the incompressible Navier–Stokes equation', *Comput. Meth. Appl. Mech. Engng.*, **32,** 199–259 (1982).
5. T. J. R. Hughes, 'A simple scheme for developing 'upwind' finite elements', *Int. J. Numer. Methods Engng.*, **12,** 1359–1365 (1978).
6. D. W. Kelly, S. Nakazawa, O. C. Zienkiewicz and J. C. Heinrich, 'A note on upwinding and anisotropic balancing dissipation in finite element approximations to convective diffusion problems', *Int. J. Numer. Methods Engng.*, **15,** 1705–1711 (1980).
7. T. J. R. Hughes and A. N. Brooks, 'A theoretical framework for Petrov–Galerkin methods with discontinuous weighting functions: applications to the streamline-upwind procedure', *Finite Elements Fluids*, **4,** 47–65 (1982).
8. T. J. R. Hughes, 'Recent progress in the development and understanding of SUPG methods with special reference to the compressible Euler and Navier–Stokes equations', *Finite Elements Fluids*, **7,** 273–287 (1987).

 

9. T. J. R. Hughes, L. P. Franca and M. Mallet, 'A new finite element formulation for computational fluid dynamics: VI. convergence analysis of the generalized SUPG formulation for linear time-dependent multidimensional advective–diffusive system', *Comput. Meth. Appl. Mech. Engng.*, **63,** 97–112 (1987).
10. T. E. Tezduyar, Y. J. Park and H. A. Deans, 'Finite element procedures for time-dependent convection–diffusion–reaction systems', *Finite Elements Fluids*, **7,** 25–45 (1987).
11. E. G. D. Do Carmo and A. C. Galeão, 'Feedback Petrov–Galerkin methods for convection-dominated problems', *Comput. Meth. Appl. Mech. Engng.*, **88,** 1–16 (1991).
12. H. M. Leismann and E. O. Frind, 'A symmetric-matrix time integration scheme for the efficient solution of advection–dispersion problems', *Water Resources Res.*, **25**(6)**,** 1133–1139 (1989).
13. S. Gärtner, Zur diskreten Approximation kontinuumsmechanischer Bilanzgleichungen, Bericht 24, Institut für Strömungsmechanik und Elektron. Rechnen im Bauwesen, Universität Hannover, 1987.
14. K.-P. Kröhn, Simulation von Transportvorgängen im klüftigen Gestein mit der Methode der Finiten Elementen, *Dissertation*, Institut für Strömungsmechanik und Elektron. Rechnen im Bauwesen, Universität Hannover, 1990.
15. P. S. Huyakorn and G. F. Pinder, *Computational Methods in Subsurface Flow*, Academic Press, San Diego, 1983.
16. C. I. Voss, 'A finite-element simulation model for saturated-unsaturated, fluid density-dependent groundwater flow with energy transport or chemically-reactive single-species solute transport', *Report* 84–4369, U.S. Geological Survey, 1984.
17. P. S. Huyakorn, B. H. Lester and J. W. Mercer, 'An efficient finite element technique for modeling transport in fractured porous media: 1. single species transport', *Water Resources Res.*, **19**(3), 841–854 (1983).
18. R. Helmig, Theorie und Numerik der Mehrphasenströmungen in geklüftet-porösen Medien, Bericht 34, Institut für Strömungsmechanik und Elektron. Rechnen im Bauwesen, Universität Hannover, 1993.
19. C. S. Carrano and G. T. Yeh, 'A Fourier analysis and dynamic optimization of the Petrov–Galerkin finite element method', *Proc. Computational Methods in Water Resources X*, Vol. 1, Heidelberg, 1994, pp. 191–198.
20. S. P. Neuman, 'Adaptive Eulerian–Lagrangian finite element method for advection–dispersion', *Int. J. Numer. Methods Engng.*, **20,** 321–337 (1984).
21. W. Kinzelbach, *Numerische Methoden zur Modellierung des Transports von Schadstoffen im Grundwasser*, Oldenburg, München. 1987.
22. R. Szymkiewicz, 'Solution of the advection–diffusion equation using the spline function and finite elements', *Commun. Numer. Meth. Engng.*, **9,** 197–206 (1993).
23. C. Blömer, 'Eine neue Diskretisierung für zweidimensionale Transportprobleme mit dominanter Konvektion', *Dissertation*, Department of Mathematics, Ruhr-Universität Bochum, 1992.
24. A. O. Garder, D. W. Peaceman and A. L. Pozzi, Jr., 'Numerical calculations of multidimensional miscible displacement by the method of characteristics', *Soc. Petrol. Engng. J.*, **4,** 26–36 (1964).
25. L. F. Konikow and L. D. Bredehoeft, 'Computer model of two-dimensional solute transport and dispersion in groundwater', *Techniques of Water-Resources Investigation*, Chapter C2, book 7, U.S. Geological Survey, Reston, 1978.
26. Y. Ijiri and K. Karasaki, 'A Lagrangian–Eulerian finite element method with adaptive gridding for advection–dispersion equation', *Proc. Computational Methods in Water Resources X* Vol. 1, Heidelberg, 1994, pp. 291–298.
27. M. A. Celia, 'Eulerian Lagrangian localized adjoint method for contaminant transport simulations', *Proc. Computational Methods in Water Resources X*, Vol 1, Heidelberg, 1994, pp. 207–216.
28. P. Binning and M. A. Celia, 'Two-dimensional Eulerian Lagrangian localized adjoint method for the solution of the contaminant transport equation in the saturated and unsaturated zones', *Proc. Computational Methods in Water Resources X*, Vol. 1, Heidelberg, 1994, pp. 165–172.
29. R. E. Ewing, H. Wang and R. C. Sharpley, 'Eulerian Lagrangian localized adjoint method for transport of nuclear-waste contaminant in porous media', *Proc. Computational Methods in Water Resources X*, Vol. 1, Heidelberg, 1994, pp. 241–248.
30. R. Hinkelmann and W. Zielke, 'A parallel 2D Lagrangian–Eulerian model for the shallow water equations', *Proc. Computing in Civil and Building Engineering*, Vol. 1, Berlin, 1995, pp. 537–543.
31. G. I. Marchuk, *Adjoint Equations and Analysis of Complex Systems*, Kluwer, Academic Publisher, Dordrecht, 1995.
32. J. J. Douglas and H.H. J. Rachford, 'On the numerical solution of heat conduction problems in two and three space variables', *Trans. Amer. Math. Soc.*, **82**(2)**,** 421–439 (1956).
33. C. König, 'Numerische Berechnung des dreidimensionalen Transports im Grundwasser', *Dissertation* Department of Civil Engineering, Ruhr-Universität Bochum, 1991.
34. J. Morshed and J. J. Kaluarachchi, 'Critical assessment of the operator-splitting technique in solving the advection–dispersion–reaction equation: 2. Monod kinetics and coupled transport', *Adv. Water Res.* **18**(2)**,** 89–100 (1995).
35. E. Wendland, 'Numerical simulation of flow and high advective solute transport in fractured porous medium', *Dissertation* (in German), Department of Civil Engineering, Ruhr-Universität Bochum, 1995.
36. F. J. Leij and J. H. Dane, 'Analytical solution of the one-dimensional advection equation and two- or three-dimensional dispersion equation', *Water Resources Res.*, **26**(7)**,** 1475–1482 (1990).


 